Signals from a scalar singlet electroweak baryogenesis

Ankit Beniwal

CoEPP and CSSM, Department of Physics,
University of Adelaide, Australia

Based on:

- A. Beniwal, M. Lewicki, J. D. Wells, M. White and A. G. Williams, *JHEP* **08** (2017) 108, [arXiv:1702.06124];
- Ongoing work with M. Lewicki, M. White and A. G. Williams.

Theory Seminar, University of Oslo, Norway
September 8, 2017

Outline

Motivation

- An imbalance between matter (baryons) and antimatter (antibaryons).
- A homogeneous and symmetric Universe $\implies$ no net asymmetry, however

$$\eta \equiv \frac{n_B - n_{\overline{B}}}{s} \approx 10^{-10}.$$

- Asymmetry must be generated *dynamically* $\rightarrow$ require *Sakharov conditions* [1]
  - C and CP violation;
  - Baryon number (B) violation;
  - Departure from thermal equilibrium.
- Electroweak baryogenesis (EWBG) is an attractive possibility $\rightarrow$ generation of asymmetry via a strong first-order electroweak phase transition (EWPT).
- All ingredients for EWBG are present in the Standard Model (SM).
- The SM alone is *not* enough to explain the asymmetry $\rightarrow$ require new physics beyond the SM (BSM).

Electroweak baryogenesis (EWBG)

- A hot, radiation-dominated early Universe with zero baryon charge and full EW symmetry, i.e., $\langle\varphi\rangle = 0$.
- When $T \lesssim 100\,\text{GeV}$ (EW scale), φ develops a VEV $\rightarrow$ EW symmetry is broken.
- Baryon asymmetry is generated when the Universe transitions from $\langle\varphi\rangle = 0$ to $\langle\varphi\rangle \neq 0$.

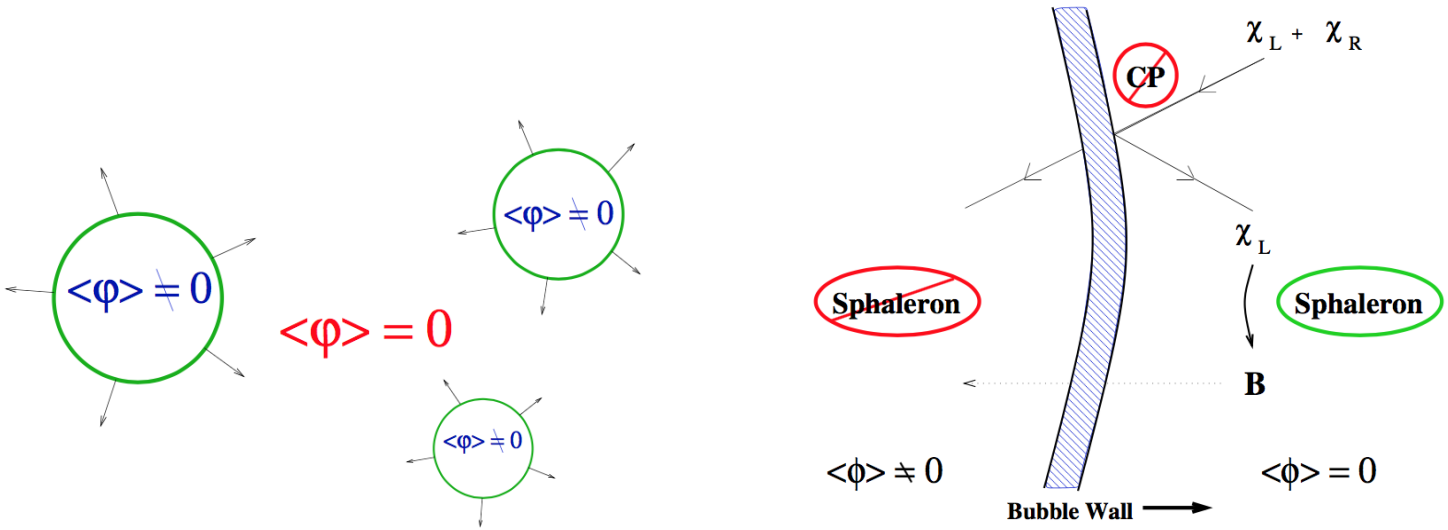

Fig. 1: *Left*: Expanding bubbles of the broken phase around the plasma in the symmetric phase. *Right*: Baryon production in front of the bubble walls. Figure from Ref. [2].

Electroweak phase transition (EWPT)

- Key ingredient is the effective potential

$$V_{\rm eff}(h,T) = V_{\rm tree}(h) + V_{\text{1-loop}}(h) + V_T(h,T).$$

- At $T = T_c$ (critical temperature), both $\langle h \rangle = 0$ and $\langle h \rangle \neq 0$ minima are *degenerate*. If a barrier exists between the two minima $\rightarrow$ a first-order phase transition, i.e.,

$$\frac{v_c}{T_c} \gtrsim 1.$$

- In the SM, $v_c/T_c \gtrsim 1$ only if $m_h \lesssim 70\,\text{GeV}$ [3] $\rightarrow$ require new BSM physics.

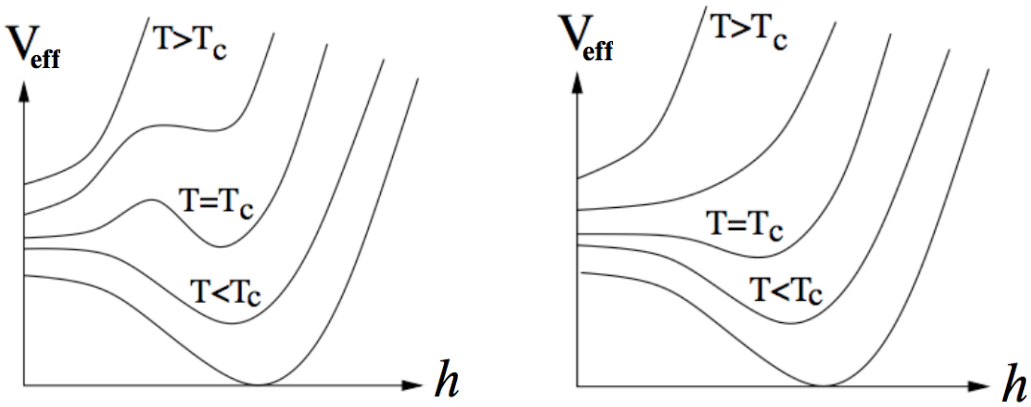

Fig. 2: Evolution of $V_{\rm eff}(h,T)$ with T for a first- (*left*) and second- (*right*) order phase transition. Figure from Ref. [4].

1. Background
   - Motivation
   - Electroweak baryogenesis (EWBG)
   - Electroweak phase transition (EWPT)

2. Recent work
   - Scalar singlet model
   - Collider signals
   - Gravitational wave signals
   - Dark Matter signals
   - Cosmological modification
   - Summary

3. Ongoing work
   - Extended scalar singlet model
   - Preliminary results
   - Future plans

Scalar singlet model

- Add a new scalar singlet S with $\mathbb{Z}_2$ symmetry $S \to -S \implies$ a DM candidate.
- Tree-level potential after EWSB is

$$V_{\text{tree}}(h, S) = -\frac{1}{2}\mu^2 h^2 + \frac{1}{4}\lambda h^4 + \frac{1}{2}\lambda_{HS} h^2 S^2 + \frac{1}{2}\mu_S^2 S^2 + \frac{1}{4}\lambda_S S^4.$$

- The physical S mass is

$$m_S^2 = \mu_S^2 + \lambda_{HS} v_0^2,$$

  where $v_0 = \mu/\sqrt{\lambda} \simeq 246\,\text{GeV} =$ SM Higgs VEV at $T = 0$.
- Large λ_{HS} generates a barrier between $\langle h \rangle = 0$ and $\langle h \rangle \neq 0$ minima $\to$ a strong first-order phase transition.
- Consider $m_S > m_h/2$ and $\lambda_{HS} \in [0.2, 4\pi]$ with $\lambda_S = 1$ [5].

Scalar singlet model

In this model, the EWPT can proceed in two ways:

- If $\mu_S^2 > 0 \implies$ a one-step phase transition, i.e.,

$$(\langle h \rangle, \langle S \rangle) = (0,0) \xrightarrow[\text{order}]{\text{first}} (v_0, 0).$$

- If $\mu_S^2 < 0 \implies$ a two-step phase transition, i.e.,

$$(\langle h \rangle, \langle S \rangle) = (0,0) \xrightarrow[\text{order}]{\text{second}} (0, \neq 0) \xrightarrow[\text{order}]{\text{first}} (v_0, 0).$$

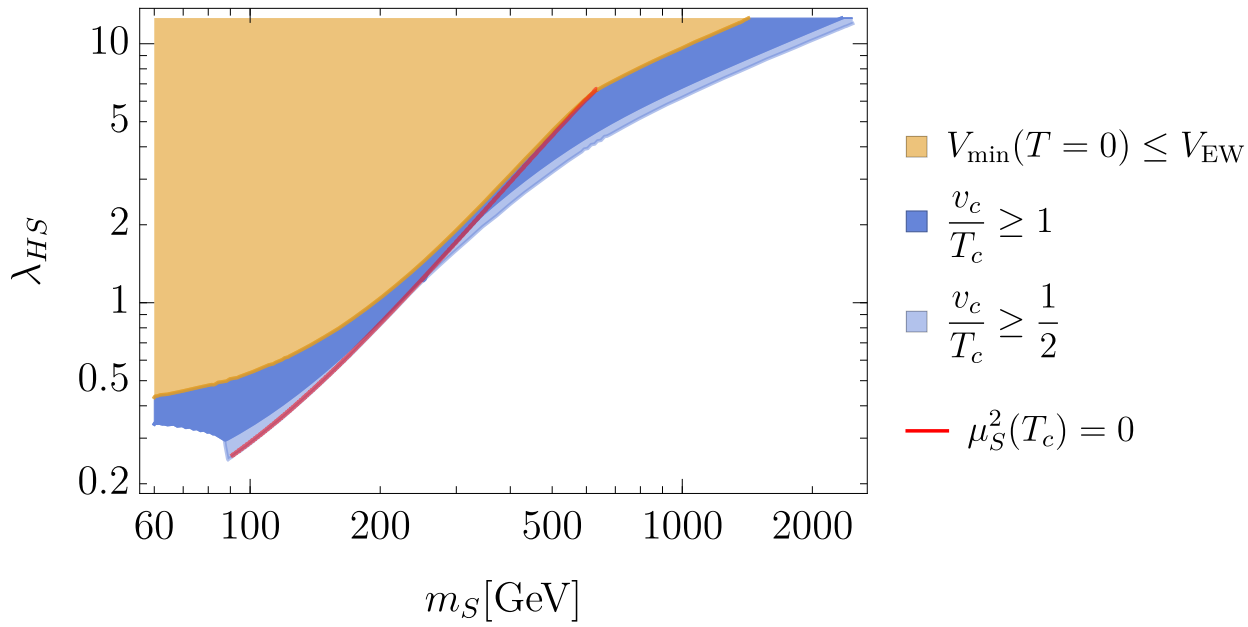

Fig. 3: Parameter space of the model relevant for EWBG. Above (below) the red curve, $\mu_S^2(T_c) < 0$ (> 0).

Collider signals

Indirect collider searches provide a far better probe for EWBG than direct searches.

1. Modification of the triple Higgs coupling
   - Given by

$$\lambda_3 = \frac{1}{6}\frac{\partial^3 V(h, S=0, T=0)}{\partial h^3}\bigg|_{h=v_0} \approx \frac{m_h^2}{2v_0} + \frac{\lambda_{HS}^3 v_0^3}{24\pi^2 m_S^2}.$$

   - Only measurable at the HL-LHC in hh production events $\rightarrow$ difficult due to a small cross section. Estimated precision is $\sim 30\%$ [6].
   - Estimated precision at 1 TeV ILC is $\sim 13\%$ with $2.5\,\text{ab}^{-1}$ [7].
   - 100 TeV collider can offer a much better precision $\rightarrow$ ignored in our analysis due to its long time frame.
2. Modification of the Zh production at lepton colliders
   - Fraction change relative to the SM value is

$$\Delta\sigma_{Zh} = \frac{1}{2}\frac{\lambda_{HS}^2 v_0^2}{4\pi^2 m_h^2}\left[1 + F\left(\frac{m_h^2}{4m_S^2}\right)\right],$$

     where

$$F(\tau) = \frac{1}{4\sqrt{\tau(\tau-1)}}\log\left(\frac{1-2\tau-2\sqrt{\tau(\tau-1)}}{1-2\tau+2\sqrt{\tau(\tau-1)}}\right).$$

   - Estimated precision at the ILC is $\sim 2\%$. FCC-ee/TLEP will probe it with $\sim 0.6\%$ accuracy at 95% C.L [8].

Collider signals

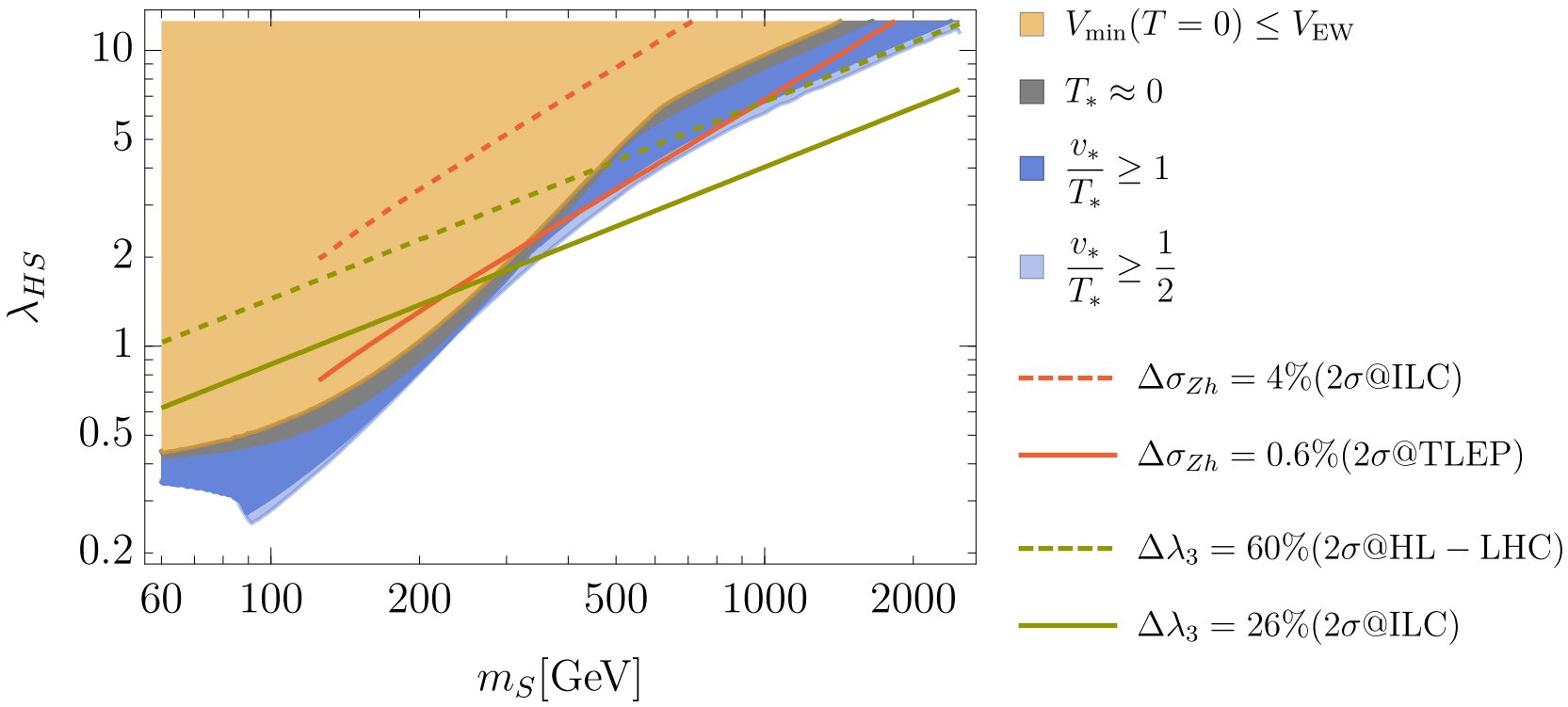

Fig. 4: Parameter space of the model relevant for EWBG along with the reach of various collider experiments. Regions above the dotted and dashed lines will be accessible at colliders. Here $\Delta\lambda_3 = (\lambda_3^{\rm SM} - \lambda_3)/\lambda_3^{\rm SM}$ and T_* is the transition temperature.

Gravitational wave signals

Three main sources of gravitational waves (GWs) from a first-order phase transition:

1. Collision of the bubble walls [9];
2. Sound waves generated after the transition [10];
3. Magneto-hydrodynamical (MHD) turbulence in the plasma [11].

All three sources depend on the following two parameters.

1. Ratio of the released latent heat to the plasma background: Defined as [12]

$$\alpha = \frac{1}{\rho_R}\left[-(V_{\rm EW} - V_f) + T\left(\frac{dV_{\rm EW}}{dT} - \frac{dV_f}{dT}\right)\right]\Bigg|_{T=T_*},$$

   where V_f = value of the potential in the unstable vacuum and T_* = transition (nucleation) temperature, i.e., when the first bubbles start to form.

2. Inverse time of the phase transition: Defined as

$$\frac{\beta}{H} = \left[T\frac{d}{dT}\left(\frac{S_3(T)}{T}\right)\right]\Bigg|_{T=T_*},$$

   where $S_3 = \mathcal{O}(3)$ symmetric action and H = Hubble rate.

Using α and β, the combined GW spectra as as a function of the frequency (f) is

$$\Omega_{\rm GW}h^2(f) = \Omega h^2_{\rm col}(f) + \Omega h^2_{\rm sw}(f) + \Omega h^2_{\rm turb}(f).$$

Gravitational wave signals

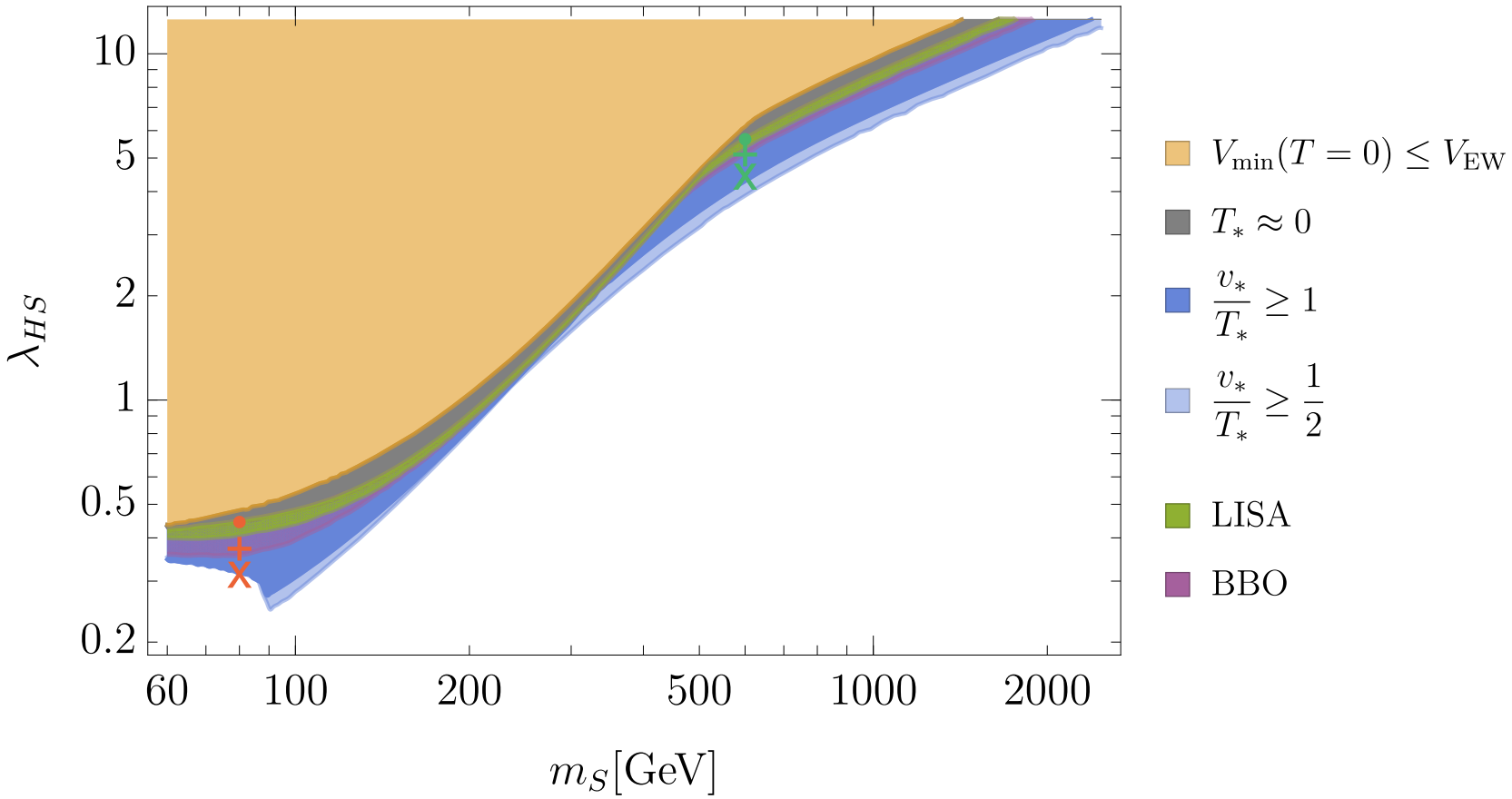

Fig. 5: Parameter space of the model relevant for EWBG along with the regions accessible at future GW detectors.

Gravitational wave signals

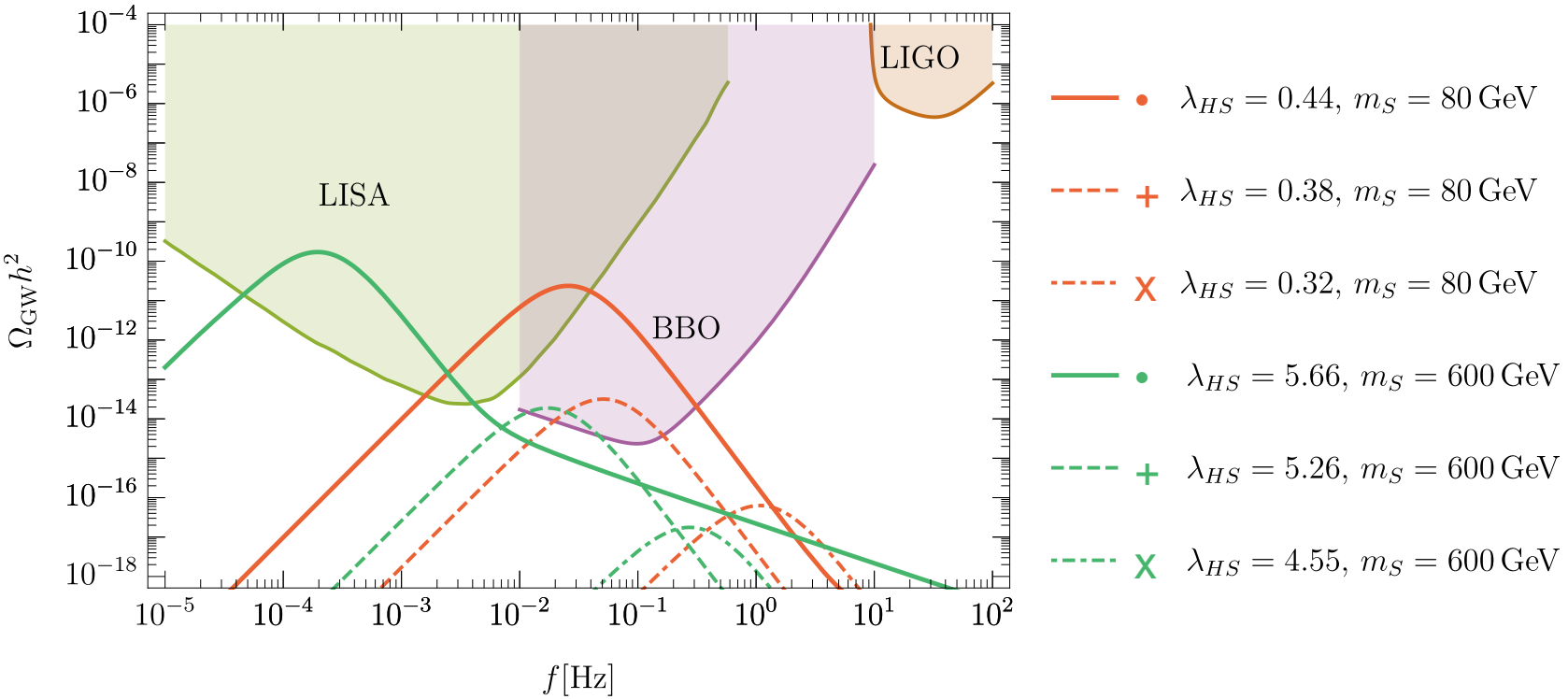

Fig. 6: Spectra of GWs from the EWPT for a few example points shown in Fig. 5. Projected sensitivities of the current and future GW detectors are also shown.

Dark Matter signals

- With $\mathbb{Z}_2$ symmetry $S \to -S$, S is a stable DM candidate.
- The S relic density must be consistent with the Planck measured value [13]

$$\Omega_{\rm DM} h^2 = 0.1188.$$

- The SI DM-nucleon cross section is

$$\sigma_{\rm SI} = \frac{\lambda_{HS}^2 f_N^2}{4\pi} \frac{\mu^2 m_n^2}{m_S^2 m_h^4},$$

  where $\mu = m_S m_n/(m_S + m_n)$, $m_n = 938.95\,\text{MeV}$ and $f_N = 0.3$ [14].
- Constraints from the LUX (2016) experiment are imposed by requiring

$$\frac{\Omega_S}{\Omega_{\rm DM}} \sigma_{\rm SI} \leq \sigma_{\rm LUX},$$

  where $\sigma_{\rm LUX}$ = 90% C.L. upper limit from LUX (2016) [15].

Dark Matter signals

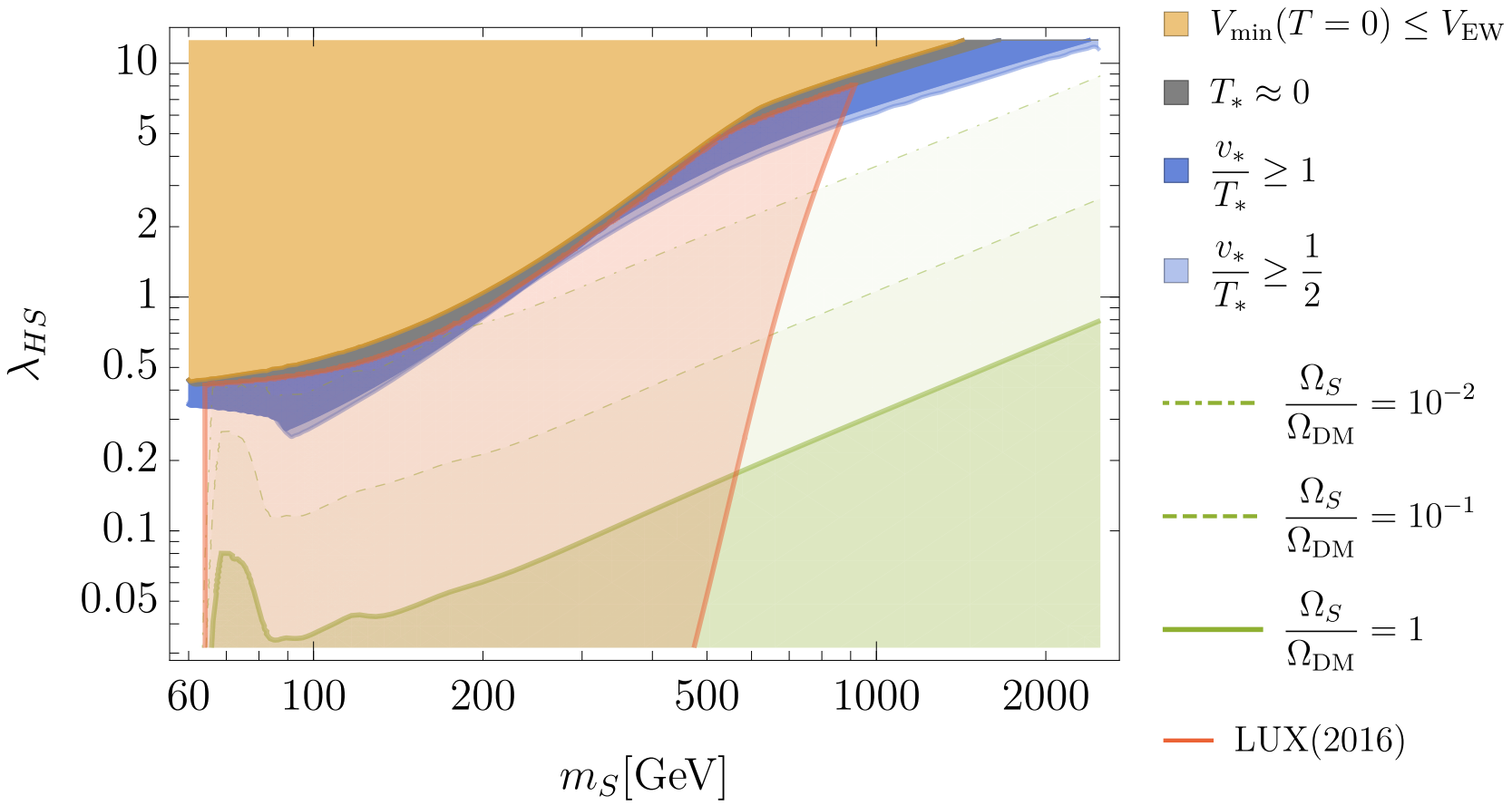

Fig. 7: Parameter space of the model relevant for EWBG along with the constraints from the DM abundance and LUX (2016) experiment. Constraints from the vacuum structure are also taken into account, hence the green and red curves do not enter into the grey and yellow shaded regions.

Cosmological modification

- Add a new component to the energy density of the early Universe $\rightarrow$ modified Friedmann equation is

$$H^2 \equiv \left(\frac{\dot{a}}{a}\right)^2 = \frac{8\pi}{3M_p^2}\left(\frac{\rho_R}{a^4} + \frac{\rho_N}{a^n}\right),$$

  where $a \equiv a(t)$ = scale factor and $n > 4 \rightarrow$ dilutes before it modifies any cosmological measurements.
- First important measurement comes from the Big Bang Nucleosynthesis (BBN) $\rightarrow$ the Hubble rate can be measured around that time.
- Observed expansion is consistent with a Universe filled with the SM radiation $\rightarrow$ within experimental uncertainties, one can add a small fraction of ρ_N.
- Translate the effective number of neutrino species into a modification of the Hubble rate

$$\left.\frac{H}{H_R}\right|_{\rm BBN} = \sqrt{1 + \frac{7}{43}\Delta N_{\nu_{\rm eff}}},$$

  where $H_R = H$ in the standard case and

$$\Delta N_{\nu_{\rm eff}} = (N_{\nu_{\rm eff}} + 2\sigma) - N_{\nu_{\rm eff}}^{\rm SM} = (3.28 + 2 \times 0.28) - 3.046 = 0.794.$$

Cosmological modification

- Assume the new component has no direct interaction with the SM, i.e.,

$$\frac{\rho_R}{a^4} = \frac{\pi^2}{30} g T^4,$$

where g = number of d.o.f. in the SM $\rightarrow$ usual result for the Hubble rate in the radiation-dominated case

$$H_R = \sqrt{\frac{4\pi}{45} g} \frac{T^2}{M_p}.$$

- Upper bound on the expansion rate at an earlier time is

$$\frac{H}{H_R} = \sqrt{\left(\frac{H}{H_R}\Big|_{\rm BBN} \right)^2 - 1} \times \left[\left(\frac{g}{g_{\rm BBN}} \right)^{1/4} \frac{T}{T_{\rm BBN}} \right]^{\frac{n-4}{2}},$$

where $T_{\rm BBN} = 1\,\text{MeV}$.

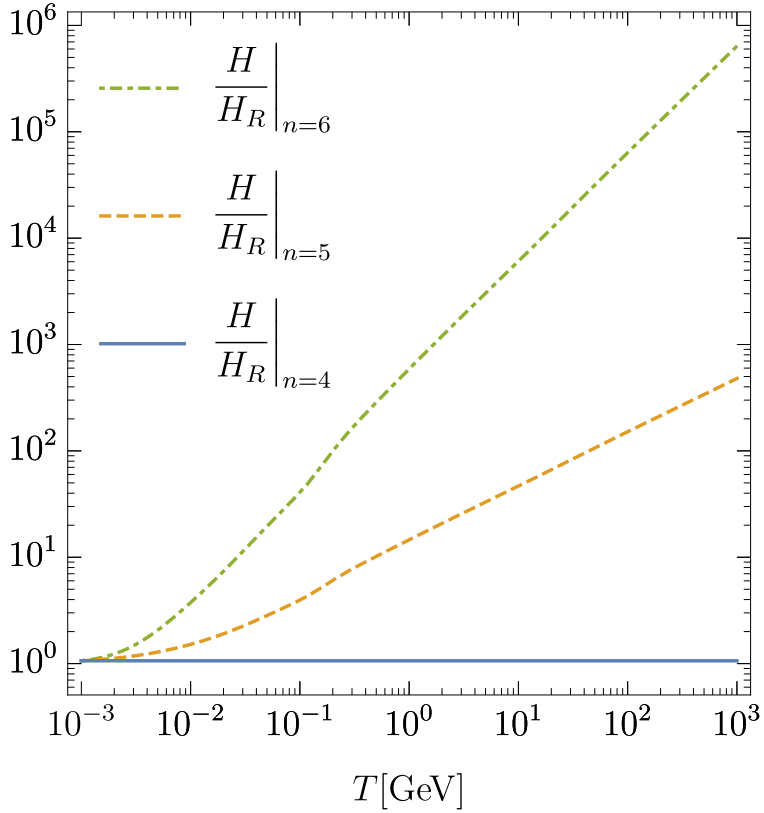

Fig. 8: Maximal modification of the Hubble rate without any conflicts with the experimental bounds.

Cosmological modification

A non-standard cosmological history can have important consequences.

- *Sphaleron bound*: Simplest criterion for the decoupling of sphalerons

$$\Gamma_{\rm Sph} = T^4 \mathcal{B}_0 \frac{g}{4\pi} \left(\frac{v}{T}\right)^7 \exp\left(-\frac{4\pi}{g}\frac{v}{T}\right) \leq H,$$

where $\mathcal{B}_0$ encapsulate the details of the $SU(2)$ sphaleron calculation.

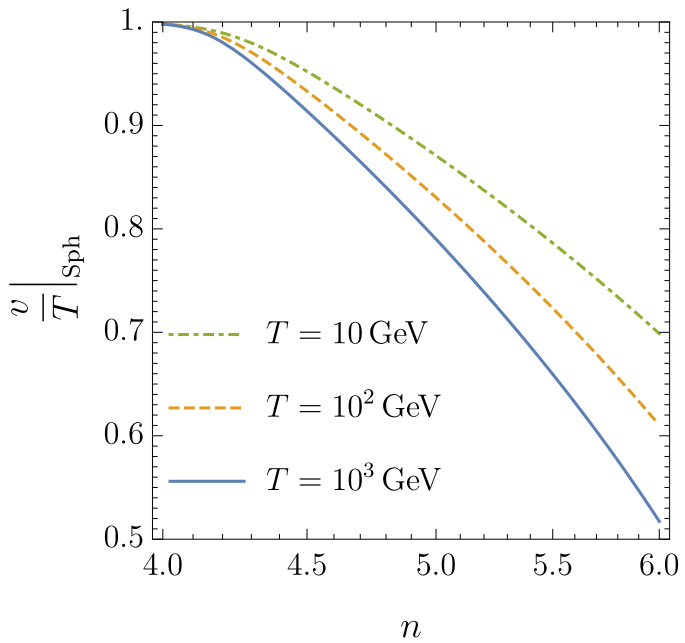

Fig. 9: Values of v/T at $T = T_*$ needed to avoid the washout of baryon asymmetry after the EWPT as function of n.

Cosmological modification

- *Dark Matter*: Increased Hubble rate $\rightarrow$ early freeze-out of S than in the standard case $\implies$ larger abundance of S in the Universe today.

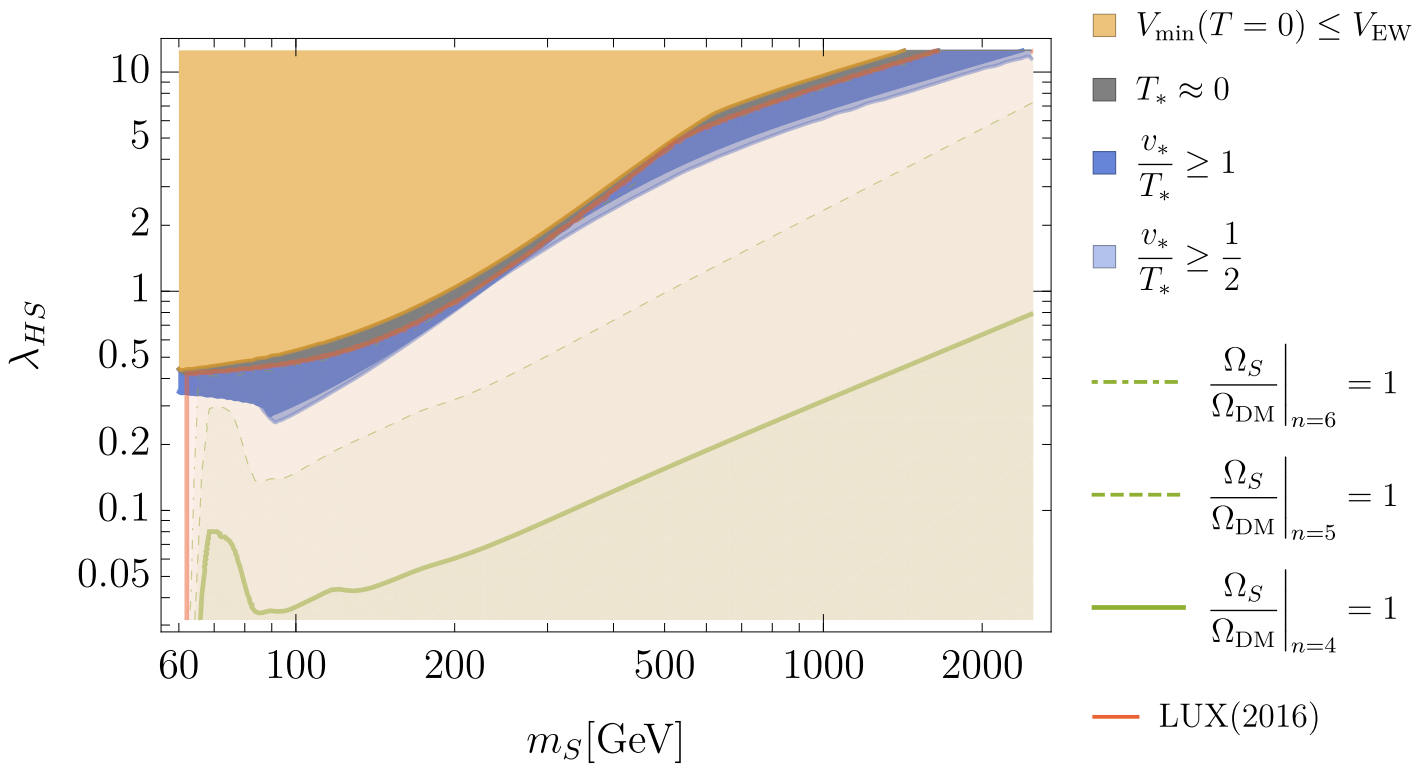

Fig. 10: Parameter space of the model relevant for EWBG along with the DM abundance and direct detection constraints due to the cosmological modification. The direct detection limits shown are based on the S abundance with $n = 6$.

Summary

- Studied the viability and detection prospects of the scalar singlet model.
- Focused on two attractive features, namely the possibility to facilitate EWBG and a DM candidate.
- Discussed various experimental probes and their reach in parts of the model parameter space, i.e., collider, gravitational and dark matter signals.
- Future gravitational wave detectors will have a better reach in accessible the parameter space relevant for EWBG than the future collider experiments.
- Correct DM abundance *cannot* be obtained simultaneously with a first-order phase transition.
- Only two regions allowing EWBG remains viable, the Higgs resonance region $m_S \sim m_h/2$ and the high mass region, $m_S \gtrsim 700\,\text{GeV}$.
- Employed a simple cosmological model which redshifts faster than radiation (i.e., $\rho_N \propto a^n$ where $n > 4$).
- Increased DM abundance from the cosmological modification is followed by severe constraints from the direct DM searches.
- All the DM constraints can be avoided if the scalar S only serves as a mediator between a new DM candidate and the SM.

Extended scalar singlet model

- Model Lagrangian is

$$\mathscr{L} = \mathscr{L}_{\rm SM} + \mathscr{L}_S + \mathscr{L}_\psi + \mathscr{L}_{\rm int},$$

where

$$\begin{aligned}
\mathscr{L}_S &= \frac{1}{2}(\partial_\mu S)(\partial^\mu S) + \frac{1}{2}\mu_S^2 S^2 + \frac{1}{3}\mu_3 S^3 - \frac{1}{4}\lambda_S S^4, \\
\mathscr{L}_\psi &= \overline{\psi}(i\partial\!\!\!/ - \mu_\psi)\psi - g_S\overline{\psi}\psi S, \\
\mathscr{L}_{\rm int} &= -\mu_{\Phi S}\Phi^\dagger\Phi S - \frac{1}{2}\lambda_{\Phi S}\Phi^\dagger\Phi S^2.
\end{aligned}$$

- Remove $-\mu_1^3 S$ term by the shift symmetry $S \to S + \sigma$.
- If $\mu_3 = \mu_{\Phi S} = g_S = 0 \implies S$ is $\mathbb{Z}_2$ symmetric $\to$ scalar Higgs portal.
- Tree-level scalar potential is modified to

$$V = V_{\rm SM} + V_S + V_{\rm int},$$

where

$$V_{\rm SM} = -\mu_\Phi^2\Phi^\dagger\Phi + \lambda_\Phi(\Phi^\dagger\Phi)^2$$

and

$$\Phi = \begin{pmatrix} G^+ \\ \frac{1}{\sqrt{2}}\left(\phi + iG^0\right) \end{pmatrix}.$$

Extended scalar singlet model

- Both ϕ and S can develop non-zero VEVs. At $T = 0$,

$$\langle\phi\rangle|_{T=0} = v_0, \quad \langle S\rangle|_{T=0} = s_0$$

such that

$$\Phi = \frac{1}{\sqrt{2}} \begin{pmatrix} 0 \\ v_0 + \varphi \end{pmatrix}, \quad S = s_0 + s.$$

- After EWSB, we get

$$\mu_\Phi^2 = \lambda_\Phi v_0^2 + \mu_{\Phi S} s_0 + \frac{1}{2}\lambda_{\Phi S} s_0^2,$$

$$\mu_S^2 = -\mu_3 s_0 + \lambda_S s_0^2 + \frac{\mu_{\Phi S} v_0^2}{2 s_0} + \frac{1}{2}\lambda_{\Phi S} v_0^2.$$

- $\mathscr{L}_{\text{int}}$ leads to a mixing between φ and $s \rightarrow$ rotate to mass-eigenstate basis

$$\begin{pmatrix} h \\ H \end{pmatrix} = \begin{pmatrix} \cos\alpha & -\sin\alpha \\ \sin\alpha & \cos\alpha \end{pmatrix} \begin{pmatrix} \varphi \\ s \end{pmatrix},$$

where α is the mixing angle.

Extended scalar singlet model

- The physical h and H masses are

$$m_h^2 = \mathcal{M}_{\varphi\varphi}^2 \cos^2\alpha + \mathcal{M}_{ss}^2 \sin^2\alpha - 2\mathcal{M}_{\varphi s}^2 \sin\alpha\cos\alpha,$$

$$m_H^2 = \mathcal{M}_{\varphi\varphi}^2 \sin^2\alpha + \mathcal{M}_{ss}^2 \cos^2\alpha + 2\mathcal{M}_{\varphi s}^2 \sin\alpha\cos\alpha.$$

- Tree-level potential must be bounded from below $\rightarrow$ require

$$\lambda_\Phi > 0, \quad \lambda_S > 0, \quad \lambda_{\Phi S} > -2\sqrt{\lambda_\Phi \lambda_S}.$$

- After EWSB, the fermion DM Lagrangian is

$$\mathscr{L}_\psi = \overline{\psi}(i\partial\!\!\!/ - m_\psi)\psi - g_S \overline{\psi}\psi s,$$

where

$$m_\psi = \mu_\psi + g_S s_0$$

is the physical fermion DM mass.

Extended scalar singlet model

- With $m_h = 125\,\text{GeV}$ and $v_0 = 246.2\,\text{GeV}$, the model contains 7 free parameters

$$\boxed{m_H, \quad s_0, \quad \mu_3, \quad \lambda_S, \quad \alpha, \quad m_\psi, \quad g_S.}$$

- Remaining parameters can be expressed as

$$\lambda_\Phi = \frac{1}{2v_0^2}\left(m_h^2 \cos^2\alpha + m_H^2 \sin^2\alpha\right),$$

$$\mu_{\Phi S} = -\frac{2s_0}{v_0^2}\left(m_h^2 \sin^2\alpha + m_H^2 \cos^2\alpha + \mu_3 s_0 - 2\lambda_S s_0^2\right),$$

$$\lambda_{\Phi S} = \frac{1}{v_0 s_0}\Big[(m_H^2 - m_h^2)\sin\alpha\cos\alpha - \mu_{\Phi S} v_0\Big],$$

$$\mu_\Phi^2 = \lambda_\Phi v_0^2 + \mu_{\Phi S} s_0 + \frac{1}{2}\lambda_{\Phi S} s_0^2,$$

$$\mu_S^2 = -\mu_3 s_0 + \lambda_S s_0^2 + \frac{\mu_{\Phi S} v_0^2}{2s_0} + \frac{1}{2}\lambda_{\Phi S} v_0^2.$$

Preliminary results

- Use `micrOMEGAs-v4.3.5` [16] to compute the fermion DM relic density and match with the Planck measured value [13], i.e., $\Omega_{\rm DM}h^2 = 0.1188$.
- Fermion DM annihilates into SM particles via an h/H exchange.

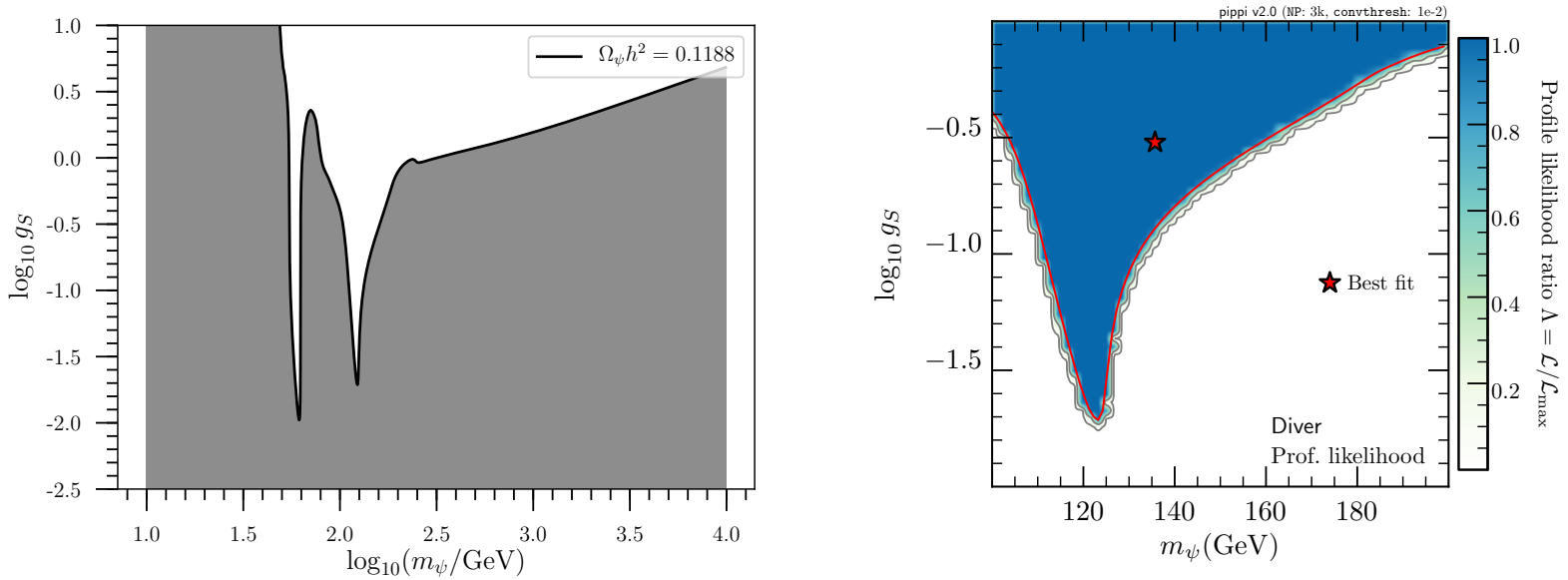

Fig. 11: *Left*: Fixed relic density contour in the (m_ψ, g_S) plane for the full mass range. *Right*: A parameter space scan of the model using `Diver-v1.0.2` [17]. In both plots, the remaining free parameters are set to $m_H = 250\,\text{GeV}$, $s_0 = \mu_3 = 300\,\text{GeV}$, $\lambda_S = 1$ and $\alpha = \pi/4$.

Preliminary results

- Fermion DM-nucleon interaction occurs via an h/H exchange in t-channel $\rightarrow$ a SI interaction.
- The SI DM-nucleon cross section is

$$\sigma_{\mathrm{SI}}^{\psi\mathcal{N}} = \frac{\mu^2}{\pi} G_{\mathcal{N}}^2,$$

where $\mathcal{N} \in (p, n)$, $\mu = m_\psi m_{\mathcal{N}}/(m_\psi + m_{\mathcal{N}})$ and

$$G_{\mathcal{N}} = \frac{g_S \sin\alpha \cos\alpha}{v_0} \left(\frac{1}{m_h^2} - \frac{1}{m_H^2} \right) m_{\mathcal{N}} f_{\mathcal{N}}.$$

- Impose limits from XENON1T (2017) [18] by requiring

$$\frac{\Omega_\psi}{\Omega_{\mathrm{DM}}} \sigma_{\mathrm{SI}}^{\psi\mathcal{N}} \leq \sigma_{\mathrm{XENON1T}}.$$

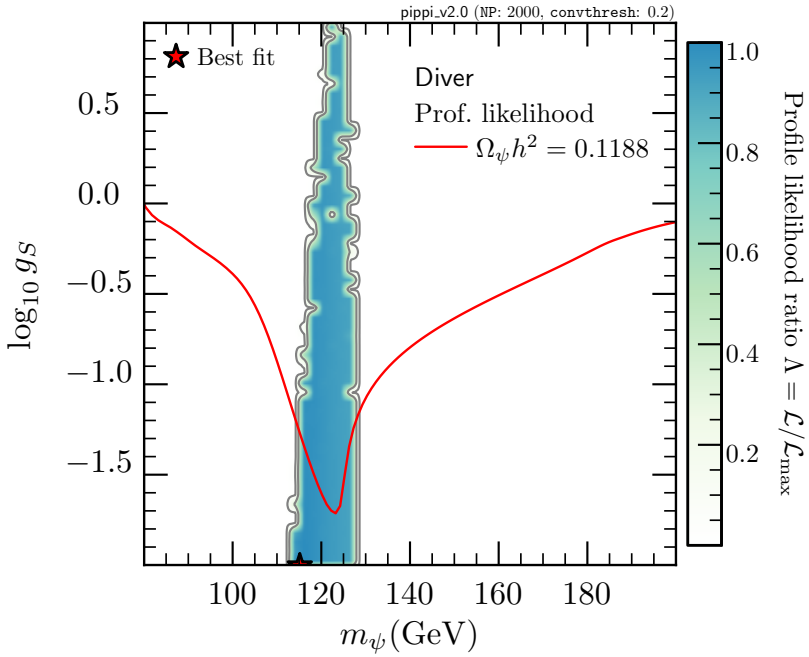

Fig. 12: Parts of the model parameter space that are consistent with the XENON1T (2017) experiment. The remaining free parameter values are same as in Fig. 11.

Preliminary results

- Find regions in the model parameter space where $v_c/T_c \gtrsim 0.6$ subject to the following constraints:

$$V_{\rm min}(T=0) \leq V_{\rm EW} \rightarrow \text{excluded;}$$
$$\lambda_{\Phi S} \leq -2\sqrt{\lambda_\Phi \lambda_S} \rightarrow \text{potential unbounded from below;}$$
$$\lambda_S \geq 4\pi,\ \lambda_\Phi \geq 4\pi,\ \lambda_{\Phi S} \geq 4\pi \rightarrow \text{non-perturbative couplings.}$$

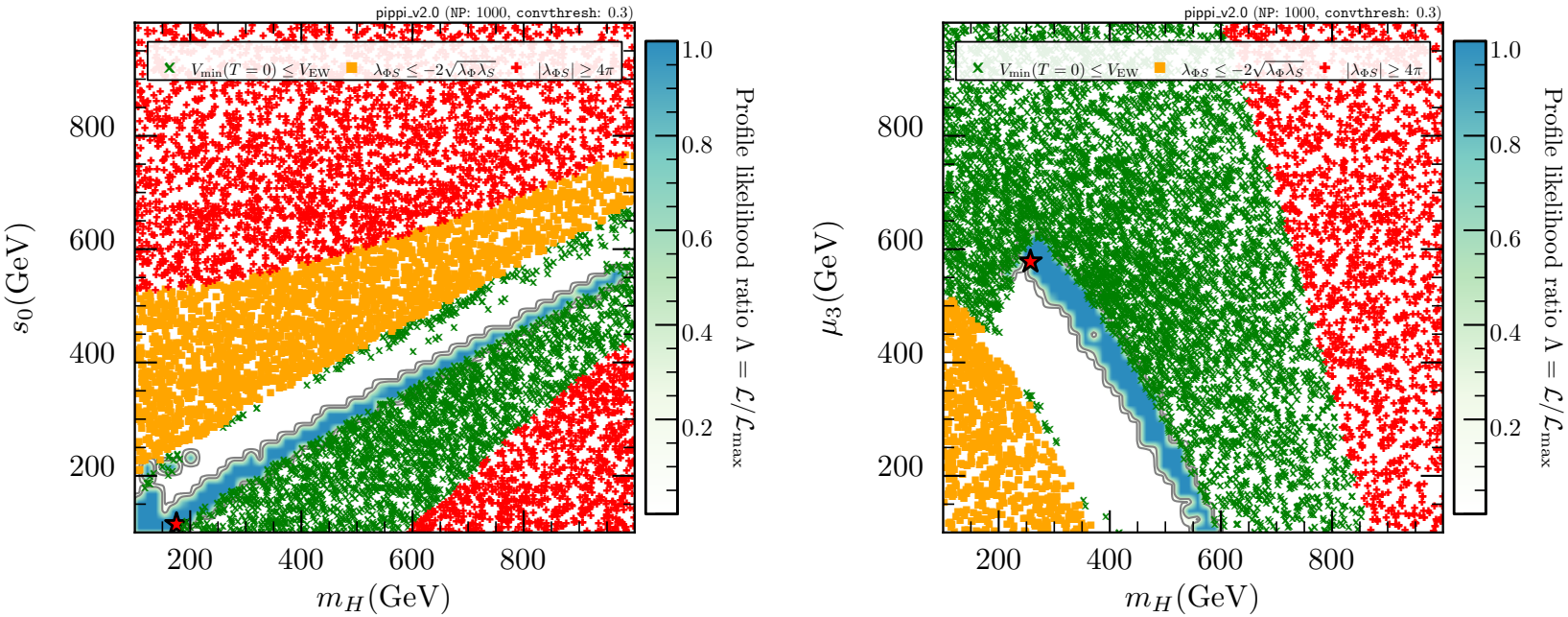

Fig. 13: Regions in the 2D parameter space where $v_c/T_c \gtrsim 0.6$ (blue shaded).

Preliminary results

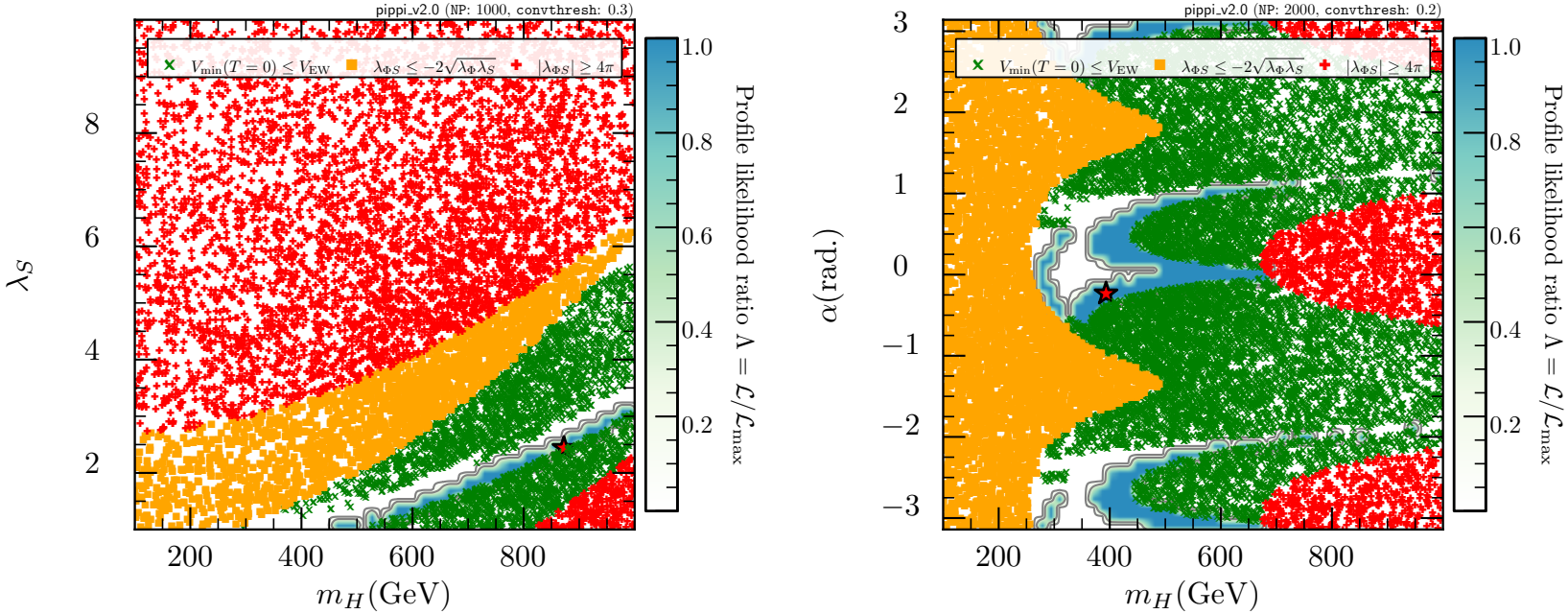

Fig. 14: Regions in the 2D parameter space where $v_c/T_c \gtrsim 0.6$ (blue shaded).

Future plans

Imposed constraints from the relic density, direct detection and electroweak baryogenesis. Yet to implement constraints from

- *Electroweak precision observables (EWPO)*
  The new scalar modifies the gauge boson self-energy diagrams $\rightarrow$ affects the oblique parameters S, T and U.
- *Collider searches*
  A mixing between φ and S leads to a modification in the signal strengths

$$\mu_h = \frac{\Gamma_h^{\rm SM} \cos^4\alpha}{\Gamma_h^{\rm SM}\cos^2\alpha + \Gamma_{h\to\overline{\psi}\psi} + \Gamma_{h\to HH}},$$

$$\mu_H = \frac{\Gamma_H^{\rm SM} \sin^4\alpha}{\Gamma_H^{\rm SM}\sin^2\alpha + \Gamma_{H\to\overline{\psi}\psi} + \Gamma_{H\to hh}}.$$

Goal: Perform a full 7D scan of the model parameter space using `Diver-v1.0.2` [17] with these constraints.

Backup slides

Effective potential

- One-loop correction to the $T = 0$ potential using the cutoff regularisation and on-shell scheme [19]

$$V_{\text{1-loop}}(h, S) = \sum_{i=h,\chi,W,Z,t,S} \frac{n_i}{64\pi^2} \left[m_i^4 \left(\log \frac{m_i^2}{m_{0i}^2} - \frac{3}{2} \right) + 2 m_i^2 m_{0i}^2 \right],$$

  where $n_{\{h,\chi,W,Z,t,S\}} = \{1, 3, 6, 3, -12, 1\}$ and $m_0 =$ particle masses at the EW VEV $h = v_0, S = 0$.

- The field-dependent masses are

$$m_W^2 = \frac{g^2}{4} h^2, \quad m_Z^2 = \frac{g^2 + g'^2}{4} h^2,$$
$$m_t^2 = \frac{y_t^2}{2} h^2, \quad m_\chi^2 = -\mu^2 + \lambda h^2 + \lambda_{HS} S^2.$$

- The h and S masses are the eigenvalues of

$$\mathcal{M}_{HS} = \begin{pmatrix} -\mu^2 + 3\lambda h^2 + \lambda_{HS} S^2 & 2\lambda_{HS} h S \\ 2\lambda_{HS} h S & \mu_S^2 + 3\lambda_S S^2 + \lambda_{HS} h^2 \end{pmatrix}.$$

Effective potential

- The finite temperature corrections are

$$V_T(h,S,T) = \sum_{i=h,\chi,W,Z,S} \frac{n_i T^4}{2\pi^2} J_b\left(\frac{m_i^2}{T^2}\right) + \sum_{i=t} \frac{n_i T^4}{2\pi^2} J_f\left(\frac{m_i^2}{T^2}\right),$$

  where

$$J_{b/f}\left(\frac{m_i^2}{T^2}\right) = \int_0^\infty dk\, k^2 \log\left[1 \mp \exp\left(-\sqrt{\frac{k^2+m_i^2}{T^2}}\right)\right].$$

- Resum the multi-loop infrared divergent contributions to boson longitudinal polarisation by adding thermal corrections to masses [20]

$$\Pi_h(T) = \Pi_\chi(T) = T^2\left(\frac{g'^2}{16} + \frac{3g}{16} + \frac{\lambda}{2} + \frac{y_t^2}{4} + \frac{\lambda_S}{12}\right),$$

$$\Pi_S(T) = T^2\left(\frac{\lambda_{HS}}{3} + \frac{\lambda_S}{4}\right), \quad \Pi_W(T) = \frac{11}{6} g^2 T^2.$$

Effective potential

- For the two scalars, the thermally corrected masses are the eigenvalues of

$$\mathcal{M}_{HS} + \begin{pmatrix} \Pi_h(T) & 0 \\ 0 & \Pi_S(T) \end{pmatrix},$$

  whereas for Z and γ, they are

$$\begin{pmatrix} \frac{1}{4}g^2h^2 + \frac{11}{6}g^2T^2 & -\frac{1}{4}g'gh^2 \\ -\frac{1}{4}g'gh^2 & \frac{1}{4}g'^2h^2 + \frac{11}{6}g'^2T^2 \end{pmatrix}.$$

- In all other cases, we substitute

$$m_i^2 \to m_i^2 + \Pi_i.$$

- The effective potential is

$$V_{\text{eff}}(h, S, T) = V_{\text{tree}}(h, S) + V_{\text{1-loop}}(h, S) + V_T(h, S, T).$$

Two-step phase transition

- Finding T_* $\equiv$ probability of finding a field configuration with action S_3 within a volume $\mathcal{V}$ [21]

$$\frac{\Gamma}{\mathcal{V}} \approx T^4 \exp\left(-\frac{S_3(T)}{T}\right),$$

where

$$S_3 = 4\pi \int dr\, r^2 \left\{ \frac{1}{2}\left(\frac{dh}{dr}\right)^2 + \frac{1}{2}\left(\frac{dS}{dr}\right)^2 + V_{\text{eff}}(h, S, T) \right\}.$$

- Parametrise the path by $\vec{\phi}(t) = (h(t), S(t))$ which connects the initial and final vacuum [22]. Set

$$\left|\frac{d\vec{\phi}}{dt}\right|^2 = \left(\frac{dh}{dt}\right)^2 + \left(\frac{dS}{dt}\right)^2 = 1$$

such that $d\vec{\phi}/dt \parallel$ path and $d^2\vec{\phi}/dt^2 \perp$ path $\rightarrow$ equations of motion (EOMs) are

$$\frac{d\vec{\phi}}{dt}\left(\frac{d^2t}{dr^2} + \frac{2}{r}\frac{dt}{dr}\right) = (\nabla V)_{\parallel},$$

$$\frac{d^2\vec{\phi}}{dt^2}\left(\frac{dt}{dr}\right)^2 = (\nabla V)_{\perp}.$$

Two-step phase transition

- For a given path, finding the bubble profile means solving

$$\frac{d^2t}{dr^2} + \frac{2}{r}\frac{dt}{dr} = \frac{dV}{dt}$$

to find $t(r)$ subject to the boundary conditions

$$\left.\frac{dt}{dr}\right|_{r=0} = 0, \quad t(r \to \infty) = V_f\,.$$

- Choose a certain initial path, obtain dt/dr along the path and calculate

$$\vec{N} = \frac{d^2\vec{\phi}}{dt^2}\left(\frac{dt}{dr}\right)^2 - (\nabla V)_\perp\,.$$

Modify the path to obtain $\vec{N} = 0$. After a few modifications, the action stabilises.

- Phase transition proceeds when at least one bubble is nucleated in every horizon volume, i.e.,

$$\int_{T_*}^{\infty}\frac{dT}{T}\,\frac{1}{H}\Gamma V_H = \int_{T_*}^{\infty}\frac{dT}{T}\left(\frac{1}{2\pi}\sqrt{\frac{45}{\pi g_{\rm eff}}}\,\frac{M_p}{T}\right)^4 \exp\left(-\frac{S_3(T)}{T}\right) = 1,$$

where H = Hubble rate, V_H = horizon volume and $g_{\rm eff}$ = effective number of d.o.f. at temperature T.

Bubble collisions

Peak frequency is [9]

$$f_{\rm col} = 16.5 \times 10^{-6} \frac{0.62}{v_b^2 - 0.1 v_b + 1.8} \frac{\beta}{H} \frac{T_*}{100} \left(\frac{g_*}{100}\right)^{1/6} \text{Hz}.$$

The energy density is

$$\Omega h^2_{\rm col}(f) = 1.67 \times 10^{-5} \left(\frac{\beta}{H}\right)^{-2} \frac{0.11 v_b^3}{0.42 + v_b^2} \left(\frac{\kappa\alpha}{1+\alpha}\right)^2 \left(\frac{g_*}{100}\right)^{-1/3} \frac{3.8\,(f/f_{\rm col})^{2.8}}{1 + 2.8\,(f/f_{\rm col})^{3.8}},$$

where the efficiency factor κ and the bubble wall velocity v_b is

$$\kappa = \frac{\alpha_\infty}{\alpha} \left(\frac{\alpha_\infty}{0.73 + 0.083\sqrt{\alpha_\infty} + \alpha_\infty}\right),$$

$$v_b = \frac{1/\sqrt{3} + \sqrt{\alpha^2 + 2\alpha/3}}{1+\alpha}.$$

For a very strong phase transition, the energy deposited into the fluid saturates to

$$\alpha_\infty = 0.49 \times 10^{-3} \left(\frac{v_*}{T_*}\right)^2.$$

Gravitational wave sources

Sound waves created in the plasma
Peak frequency is [10]

$$f_{\rm sw} = 1.9 \times 10^{-5} \frac{\beta}{H} \frac{1}{v_b} \frac{T_*}{100} \left(\frac{g_*}{100}\right)^{1/6} \text{Hz}.$$

The energy density is

$$\Omega h^2_{\rm sw}(f) = 2.65 \times 10^{-6} \left(\frac{\beta}{H}\right)^{-1} \left(\frac{\kappa\alpha}{1+\alpha}\right)^2 \left(\frac{g_*}{100}\right)^{-1/3} v_b \left(\frac{f}{f_{\rm sw}}\right)^3 \left(\frac{7}{4+3\left(f/f_{\rm sw}\right)^2}\right)^{7/2}.$$

MHD turbulence in the plasma
Peak frequency is [12]

$$f_{\rm turb} = 2.7 \times 10^{-5} \frac{\beta}{H} \frac{1}{v_b} \frac{T_*}{100} \left(\frac{g_*}{100}\right)^{1/6} \text{Hz}.$$

The energy density is

$$\Omega h^2_{\rm turb}(f) = 3.35\times10^{-4} \left(\frac{\beta}{H}\right)^{-1} \left(\frac{\epsilon\kappa\alpha}{1+\alpha}\right)^{3/2} \left(\frac{g_*}{100}\right)^{-1/3} v_b \frac{\left(f/f_{\rm turb}\right)^3 \left(1+f/f_{\rm turb}\right)^{-11/3}}{\left[1+8\pi f a_0/(a_* H_*)\right]}$$

where $a_*(H_*)$ = scale (Hubble) factor at $T = T_*$ and $\epsilon \approx 0.05$ = efficiency factor.

References I

[1] A. D. Sakharov, *Violation of CP Invariance, c Asymmetry, and Baryon Asymmetry of the Universe*, *Pisma Zh. Eksp. Teor. Fiz.* **5** (1967) 32–35.

[2] D. E. Morrissey and M. J. Ramsey-Musolf, *Electroweak baryogenesis*, *New J. Phys.* **14** (2012) 125003, [1206.2942].

[3] A. Bochkarev and M. Shaposhnikov, *Electroweak production of baryon asymmetry and upper bounds on the higgs and top masses*, *Modern Physics Letters A* **02** (1987) 417–427, [http://www.worldscientific.com/doi/pdf/10.1142/S0217732387000537].

[4] J. M. Cline, *Baryogenesis*, in *Les Houches Summer School - Session 86: Particle Physics and Cosmology: The Fabric of Spacetime Les Houches, France, July 31-August 25, 2006*, 2006. hep-ph/0609145.

[5] A. Beniwal, F. Rajec, C. Savage, P. Scott, C. Weniger, M. White et al., *Combined analysis of effective Higgs portal dark matter models*, *Phys. Rev. D* **93** (2016) 115016, [1512.06458].

[6] F. Goertz, A. Papaefstathiou, L. L. Yang and J. Zurita, *Higgs Boson self-coupling measurements using ratios of cross sections*, *JHEP* **06** (2013) 016, [1301.3492].

[7] D. M. Asner et al., *ILC Higgs White Paper*, in *Proceedings, Community Summer Study 2013: Snowmass on the Mississippi (CSS2013): Minneapolis, MN, USA, July 29-August 6, 2013*, 2013. 1310.0763.

[8] S. Dawson et al., *Working Group Report: Higgs Boson*, in *Proceedings, 2013 Community Summer Study on the Future of U.S. Particle Physics: Snowmass on the Mississippi (CSS2013): Minneapolis, MN, USA, July 29-August 6, 2013*, 2013. 1310.8361.

[9] S. J. Huber and T. Konstandin, *Gravitational Wave Production by Collisions: More Bubbles*, *JCAP* **0809** (2008) 022, [0806.1828].

[10] M. Hindmarsh, S. J. Huber, K. Rummukainen and D. J. Weir, *Gravitational waves from the sound of a first order phase transition*, *Phys. Rev. Lett.* **112** (2014) 041301, [1304.2433].

[11] C. Caprini, R. Durrer and G. Servant, *The stochastic gravitational wave background from turbulence and magnetic fields generated by a first-order phase transition*, *JCAP* **0912** (2009) 024, [0909.0622].

[12] C. Caprini et al., *Science with the space-based interferometer eLISA. II: Gravitational waves from cosmological phase transitions*, *JCAP* **1604** (2016) 001, [1512.06239].

[13] Planck collaboration, P. A. R. Ade et al., *Planck 2015 results. XIII. Cosmological parameters*, *Astron. Astrophys.* **594** (2016) A13, [1502.01589].

References II

[14] J. M. Cline, K. Kainulainen, P. Scott and C. Weniger, *Update on scalar singlet dark matter*, *Phys. Rev. D* **88** (2013) 055025, [1306.4710].

[15] LUX collaboration, D. S. Akerib et al., *Results from a search for dark matter in the complete LUX exposure*, *Phys. Rev. Lett.* **118** (2017) 021303, [1608.07648].

[16] G. Blanger, F. Boudjema, A. Pukhov and A. Semenov, *micrOMEGAs4.1: two dark matter candidates*, *Comput. Phys. Commun.* **192** (2015) 322–329, [1407.6129].

[17] GAMBIT Scanner Workgroup collaboration, G. Martinez, D., J. McKay, B. Farmer, P. Scott, E. Roebber et al., *Comparison of statistical sampling methods with ScannerBit, the GAMBIT scanning module*, 1705.07959.

[18] XENON collaboration, E. Aprile et al., *First Dark Matter Search Results from the XENON1T Experiment*, 1705.06655.

[19] D. Curtin, P. Meade and C.-T. Yu, *Testing Electroweak Baryogenesis with Future Colliders*, *JHEP* **11** (2014) 127, [1409.0005].

[20] P. B. Arnold and O. Espinosa, *The Effective potential and first order phase transitions: Beyond leading-order*, *Phys. Rev. D* **47** (1993) 3546, [hep-ph/9212235].

[21] A. D. Linde, *Decay of the False Vacuum at Finite Temperature*, *Nucl. Phys. B* **216** (1983) 421.

[22] C. L. Wainwright, *CosmoTransitions: Computing Cosmological Phase Transition Temperatures and Bubble Profiles with Multiple Fields*, *Comput. Phys. Commun.* **183** (2012) 2006–2013, [1109.4189].